

# Surface Functionalization by Decal-like Transfer of Thermally Cross-Linked Urushiol Thin Films

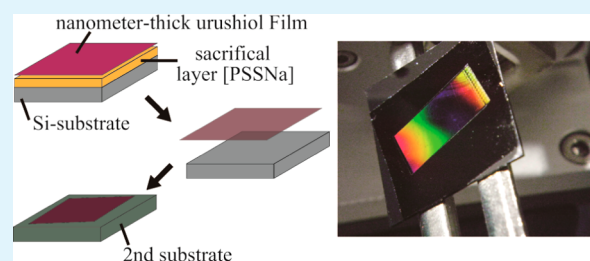
Hirohmi Watanabe,<sup>\*,†,‡</sup> Aya Fujimoto,<sup>†</sup> and Atsushi Takahara<sup>\*,†,‡</sup>

<sup>†</sup>Japan Science and Technology Agency (JST), ERATO Takahara Soft Interfaces Project, Kyushu University, 744 Motoooka, Nishi-ku, Fukuoka 819-0395, Japan

<sup>‡</sup>Institute for Materials Chemistry and Engineering, Kyushu University, 744 Motoooka, Nishi-ku, Fukuoka 819-0395, Japan

## S Supporting Information

**ABSTRACT:** We have demonstrated surface functionalization through the decal-like transfer of thermally cross-linked urushiol thin films onto various substrates. Tensile adhesive strength measurements showed that the film adheres strongly to the surface of various substrates including chemically inert materials, such as polyolefins and thermosetting resins, because of the properties of urushiol. Furthermore, the highly cross-linked structure of urushiol made the films mechanically robust. These two properties allowed the fabrication of practicable thin films for indirect surface modification. Actually, the robust thin film served as a scaffold for an Au thin film, which was then bound to various substrates. Surface-texturing of nanodecal was also demonstrated as an application aspects.



**KEYWORDS:** urushiol, thin film, adhesion, cross-linked structure, surface modification, nanodecal

## 1. INTRODUCTION

The characteristics of soft materials are strongly influenced by the physical properties of their surfaces and interfaces.<sup>1</sup> Therefore, various methods have been used to control surface topography and chemical composition, including self-assembled monolayers,<sup>2</sup> electrochemical deposition,<sup>3</sup> plasma treatment,<sup>4</sup> and other techniques.<sup>5–7</sup> In addition, we have recently demonstrated that surfaces can be functionalized by a simple decal-like transfer of free-standing, nanometer thick polymer films (Figure 1a).<sup>8,9</sup> We fabricated a cross-linked polymer thin film and found that its wetting properties were preserved after the film was attached to various substrates. Crucially, this did not require adhesive. This feature of our method widens the

variety of substrates for surface functionalization. We call this method for indirect, material-independent surface functionalization the nanodecal technique. In addition to adhesion, robustness is an important physical characteristic for practical applications of nanodecals. Otherwise, nanodecals would be easily damaged while in use. Cross-linked materials can be used to produce films that are more robust.<sup>10–12</sup>

Incidentally, material-independent surface functionalization using thin film coatings of catechol derivatives has been widely investigated. Catechol derivatives, such as polydopamine (PDA), strongly adhere to various surfaces through hydrogen bonding and chelation.<sup>13–15</sup> Kohri and co-workers reported an approach similar to ours for fabricating a free-standing polymer brush film using a PDA thin layer.<sup>16</sup> They grafted poly(2-hydroxyethyl methacrylate) from cross-linked PDA, and the thin film adhered to a Si substrate. Unfortunately, the contribution of PDA underlayer to the adhesion characteristics was unclear, because they focused on the fabrication of the transferable polymer brushes. However, the excellent adhesive properties of catechol derivatives could also be used for indirect surface functionalization using nanodecals.

Catechol compounds are found in oriental lacquer, known as urushi, which is a natural resin traditionally used for coating wood or paper substrates (Figure 1b).<sup>17–20</sup> The resin is tapped simply and permanently from a lacquer tree (binomial name: *Toxicodendron vernicifluum*), and urushi is regarded as a

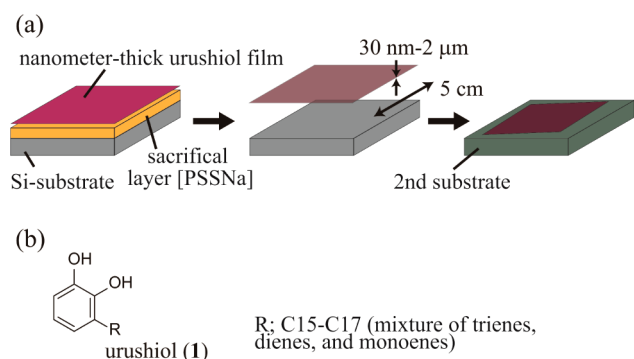


**Figure 1.** (a) Schematic illustration of the decal-like transfer of thin films, and (b) chemical structure of urushiol.

**Received:** March 29, 2014

**Accepted:** October 3, 2014

**Published:** October 3, 2014

renewable resource by the cultivation. Because urushiol, which is the main component of urushi, has double bonds in its long side chain, a highly cross-linked structure can be formed by either oxidative polymerization or thermal treatment. We have demonstrated that the long hydrocarbon side chain makes it more mechanically robust than PDA.<sup>21–23</sup> In the present study, we have fabricated thermally cross-linked urushiol nanodecals that show superior adhesion and mechanical robustness. The fabrication of nanodecals from biobase material is meaningful to establish a sustainable living. The adhesion and mechanical properties were evaluated by tensile adhesive strength and strain-induced elastic buckling tests, respectively. Moreover, surface nanotexturing and metal layer deposition were performed on these nanodecals to demonstrate potential practical applications.

## 2. EXPERIMENTAL SECTION

**2.1. Materials.** Raw urushi lacquer was purchased from Kanwa-do Urushi Club Co. Ltd., Shiga, Japan. Urushiol was extracted from the raw urushi lacquer according to our previously published method. (*Caution:* uncured urushiol can cause an allergic skin rash on contact and should be handled carefully.)<sup>21</sup> Iron(II) acetate was obtained from Acros Organics. Monodisperse polystyrene (PS) was purchased from Polyscience. The weight-average molecular weight ( $M_w$ ) and the polydispersity index ( $M_w/M_n$ ) were  $1.15 \times 10^5$  and 1.04, respectively. UV-curable photopolymer NIAC23 was obtained from Daicel Chemical Industries, Ltd. NIAC23 is a mixture of multifunctional acrylate monomer, acrylic copolymer having acrylic groups on side chains, and a small amount of a radical photoinitiator. Solvents were purchased from Kanto Chemicals and used without further purification. Octadecyltrimethoxysilane (ODTMS) was purchased from Gelest, and the surface of a Si wafer was modified with ODTMS according to a literature procedure.<sup>24</sup>

**2.2. Preparation Procedure of Nanodecals.** The thermally cross-linked urushiol nanodecal was fabricated as follows: Urushiol was first dissolved in ethanol. Iron(II) acetate was then added to the solution; the color of solution changed from light brown to black after this process. The iron(II) acetate concentration was fixed as 0.5 mol equiv against urushiol. The solution was diluted by propylene glycol monomethyl ether acetate as necessary. For example, the thickness of the urushiol nanodecal was 75 nm when the concentration of urushiol was 120 mM. The solution was homogenized by using Branson Sonifier ultrasonic cell disruptors prior to spin-coating.<sup>21</sup> Then, the solution was spin-coated on a PSSNa layer-coated Si wafer at 3000 rpm for 60 s. PSSNa layer-coated Si wafers were preliminary prepared by the spin-coating of poly(sodium styrenesulfonate) (PSSNa;  $M_w = 8.1 \times 10^3$ ) on a vacuum UV (VUV)-treated Si wafer. The thickness of the water-soluble PSSNa layer was about 1.0  $\mu\text{m}$  thick.<sup>8</sup> After thermal treatment at 100 °C for 10 min, the urushiol layer was detached from the substrate by immersing the sample in water to dissolve the PSSNa. Finally, the thin film on the water surface was reattached onto other substrates by scooping out the thin film from the water, and drying it in the air.

The PDA nanodecal was fabricated as follows: First, poly(4-hydroxystyrene) (PHS;  $M_w = 2.0 \times 10^4$ ) was spin-coated on a vacuum UV (VUV)-treated Si wafer at 3000 rpm for 60 s to give a 0.1  $\mu\text{m}$  thick sacrificial layer. Then, the sample was soaked for 24 h in a dilute aqueous solution of 3,4-dihydroxyphenethylamine hydrochloride containing 10 mM tris(hydroxymethyl)aminomethane (TRIS buffer, pH 8.5). After the rinse with pure water for three times, the sample was immersed in ethanol to dissolve the PHS.

The PS and NIAC23 nanodecal was fabricated as follows: The corresponding solutions were spin-coated on PSSNa layer-coated Si wafers. Thermal annealing at 120 °C for 10 min and photocuring by UV light irradiation for 3 min were conducted for PS and NIAC23 nanodecal, respectively. Detachment and reattachment was done using the same procedure as that for the fabrication of the urushiol nanodecal.

**2.3. Surface Nanotexturing.** A Si mold was brought into contact with an urushiol liquid film on a PSSNa layer-coated Si wafer, and the sample was pressed under a static pressure of 2.5 kN for 20 s with a NM-0501-T nanoimprinter (Meisho Kiko, Co., Ltd.). The sample was heated to 100 °C for 10 min under pressure in air. The surface topography of the Si-mold was replicated on the cured urushiol thin film after it was released from the Si mold. The Si molds for nanoimprinting were fabricated by photolithography. Before use, the surfaces of the Si molds were coated with a mold-release agent (Durasurf-DS5100, Harves Co., Ltd.).

**2.4. Adhesion Strength Measurements.** **2.4.1. Standard Test Methods for Measuring Adhesion by Tape Test.** A tape test was done according to the ASTM D3359 test procedure.<sup>23</sup> The transferred films were first cut with a razor blade to be a cross-hatch pattern. Then, a tape (3M Scotch Tape #810) was applied to the cross-hatch area followed by pulling the tape back off. The cross-hatched test area was visually compared to ASTM D3359. There were six classes of adhesion, from 5B (highest) to 0B (lowest level).

**2.4.2. Pull-off Adhesion Test.** Adhesion strength measurements were performed with a laboratory-built pull-off adhesion tester (Figure S1, Supporting Information).<sup>25</sup> A glass sphere ( $\phi = 4.76$  mm) on top of the probe was bonded to the thin film with an epoxy adhesive (Epoxy Bond Quick 5, Konishi) consisting of a mixture of epoxy resin and polyfunctional thiol acrylate monomer. The bonding of the epoxy adhesive with the film did not affect the adhesion (see the Supporting Information for details). The load during the vertical pull was detected by a high-sensitivity load cell (LC4101-G600, A&D Co., Ltd.). The speed was maintained at 20  $\mu\text{m/s}$  by a pulse motor stage (SGSP80-20ZF, Sigma Koki Co., Ltd.). The tensile adhesive strength,  $F$  ( $\text{MPa} = \text{N}/\text{mm}^2$ ), was calculated with

$$\text{tensile adhesive strength } F \text{ (MPa)} = \frac{f}{A} \quad (1)$$

Here,  $f$  is the breaking load (N) and  $A$  is the area of adhesion ( $\text{mm}^2$ ). The area of adhesion was determined by using an optical microscope (Observer A1m, Zeiss Co., Ltd.). The samples were dried under vacuum for 1 day prior to the measurements. During the measurements, the temperature and the relative humidity were kept at  $24 \pm 0.5$  °C and  $40 \pm 5\%$ , respectively. A typical example of the raw loading data and an optical microscope image of the probe are shown in Figure S2 (Supporting Information).

**2.5. Other Measurements.** UV–vis absorption spectra were recorded on a UV–vis spectrophotometer (UV-3500PC, Shimadzu). Atomic force microscopy (AFM; 5500, Agilent) was performed in noncontact AC mode with a rectangular 160  $\mu\text{m}$  cantilever (OMCL-AC160TS-W2, Olympus). The spring constant of the cantilever was 42  $\text{N m}^{-1}$ . Scanning electron microscopy (SEM) observations were performed using a Keyence VE7800. The static water contact angle (CA) was measured using a contact angle measurement system (DSA10, Krüss) equipped with an automatic liquid dispenser and a monochromatic CCD camera. During the CA measurements, temperature and humidity were controlled at 23.5 °C and 60%, respectively. The Young's modulus of the material was determined by strain-induced elastic buckling instability for mechanical measurements (SIEBIMM). This technique measures the buckling instability that occurs in a bilayer consisting of a stiff, thin-film layer and a relatively soft, thick substrate layer (Figure S3, Supporting Information).<sup>26</sup> For the electrochemical measurements, an Au layer was deposited on the film by vacuum deposition (SV-9425, SANVAC Corp.) prior to the decal-like transfer. Then, samples were transferred to the surface of an indium tin oxide (ITO)-coated glass slide (8–12  $\Omega/\text{cm}^2$  surface resistivity, Aldrich). Ag electrodes (1 mm  $\phi$ ) were formed to the top of the nanodecal to be a metal/insulator/semiconductor (MIS) stack (Ag/nanodecal/ITO). Leakage current measurements were carried out for the MIS capacitors with a potentiostat/galvanostat system (E5272A, Agilent Technologies; Parametric Measurement Solutions).<sup>10</sup>

### 3. RESULTS AND DISCUSSION

**3.1. Physical Properties of Nanodecals.** Cross-linked urushiol thin films were obtained by spin-coating and curing at 100 °C for 10 min. The film was then detached from the original substrate and was freestanding on the water surface. The film was removed from the water and attached to the substrate. The thickness of the film was varied from several nanometers to several micrometers by changing the spin-coating conditions. This is a big advantage of urushiol thin film, unlike other PDA thin films in which the film thickness is limited to several tens of nanometers due to the restriction of preparation procedure.<sup>27,28</sup> Figure 2 shows the UV absorption

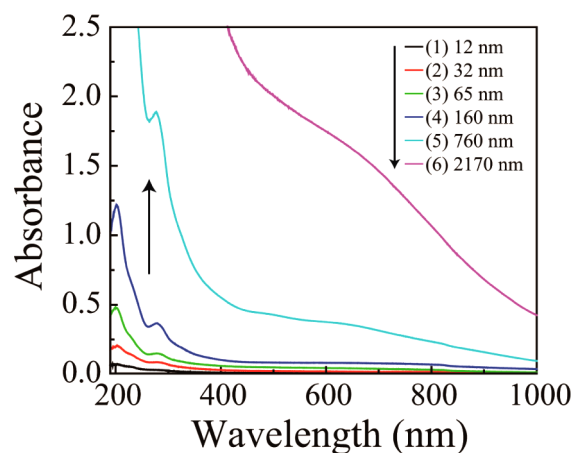


**Figure 2.** UV-vis absorption spectra of urushiol thin films after the transfer to quartz plate.

spectra of urushiol thin films attached to a quartz plate. The absorption in the visible region originated from a ligand-to-metal charge-transfer band. The monotonic increase of the absorption in the visible region with the thickness indicates that the transparency of the decal can be tuned by changing the thickness of the film. The transmittance of the films was over 80% in the visible region when the film was less than 180 nm thick. However, the transmittance was below 3% when the film was more than 2  $\mu\text{m}$  thick.

Subsequently, the physical characteristics of cross-linked urushiol thin films were evaluated. The AFM observations revealed that the surface roughness of 50 nm thick nanodecal was  $\sim 1.3$  nm with root-mean-square (RMS) roughness of within a  $5 \times 5 \mu\text{m}$  area (Figure S4, Supporting Information). SEM observations also confirmed that the film was flat and did not contain pinholes and defects (Figure S5, Supporting Information). Thicker nanodecals also showed similar surface morphology. The static water contact angle and Young's modulus of the nanodecal were  $63^\circ$  and  $0.8 \pm 0.1$  GPa,

respectively. Table 1 summarizes the physical properties of the cross-linked urushiol thin films and those of PS and NIAC23 thin films. Cracks were frequently observed during the SIEBIMM experiments for the PS thin film, whereas the cross-linked urushiol thin films did not crack, even when buckling was achieved under 10% compression. The mechanical robustness of the cross-linked urushiol thin films probably arose from these characteristics of urushiol.<sup>21</sup> Cross-linking of urushiol is done by oxidative oligomerization of catechol moiety and the following thermal Diels–Alder cycloaddition and/or addition reaction of double bonds in the side chain to form network structure. The highly cross-linked structure and the flexibility owing to the long alkyl side chain impart the robustness. Cross-linked NIAC23 thin film also showed good mechanical properties. It is worth noting that PDA thin film easily fragmented into small pieces during the detachment process to be a free-standing (Figure S6, Supporting Information). PDA was too brittle for use as a nanodecal because of the lack of the flexible side chain.<sup>23</sup> Moreover, the rough surface of PDA nanodecal (Figure S7, Supporting Information) also unfavorable for nanodecal because it provides the roughness-induced small contact area to weaken the adhesion strength.<sup>9</sup>

**3.2. Adhesion Properties of Urushiol Nanodecal.** The adhesion strength of nanodecals was evaluated qualitatively by the tape test using standard test methods for measuring adhesion (ASTM D3359). The 50 nm thick cross-linked urushiol nanodecal adhered strongly to the VUV-treated Si wafer, glass, PS plate, and copper plate, and no delamination was observed on these substrates. The nanodecal even adhered to inert polyolefins surfaces, such as polyethylene and polypropylene. The hydrophobic side chains may play an important role for the adhesion.<sup>29</sup> However, the nanodecal was delaminated from hydrophobic substrates such as poly(tetrafluoroethylene) and ODTMS-modified Si substrate. This may be because of the weak interaction with the substrates, as discussed later. The delamination from ceramics may arise from the roughness-induced small contact area.<sup>9</sup> PS nanodecal and NIAC23 nanodecal showed similar results (Table S1, Supporting Information). Adhesion strength of PDA nanodecal was unmeasurable because small pieces less than 5  $\text{mm}^2$  were only obtained due to the fragmentation.

To clarify the dependence of adhesion strength on substrates, the adhesion strength on VUV-treated Si wafer and ODTMS-modified Si substrate was quantitatively measured with a laboratory-built pull-off adhesion tester. Both substrates were flat with different contact angle (Table S1, Supporting Information). When a 50 nm thick cross-linked urushiol thin film was attached the VUV-treated Si substrate (hydrophilic substrate), an interfacial fracture between the glass sphere and the epoxy adhesive was visible in every sample (Figure 3).

**Table 1.** Physical Properties of Thin Films

sample	thickness (nm) <sup>a</sup>	roughness (nm) <sup>a,b</sup>	contact angle (deg) <sup>c</sup>	Young's modulus (GPa) <sup>d</sup>	peeling strength (MPa) <sup>e</sup>	
					VUV	ODTMS
cross-linked urushiol	50	1.3	63	$0.8 \pm 0.1$	$>6.2^g$	1.12
	1050	1.4	62	$0.8 \pm 0.1$	$>6.2^g$	0.87
PS	60	0.2	89	$1.9 \pm 0.3^f$	$>4.2^h$	1.28
NIAC23	36	0.2	59	$2.6 \pm 0.2$	$>6.2^g$	0.64

<sup>a</sup>Determined by AFM. <sup>b</sup>RMS value. <sup>c</sup>Static water contact angle. <sup>d</sup>Determined by SIEBIMM. <sup>e</sup>Determined by pull-off adhesion tester. <sup>f</sup>Cracks formed during compression. <sup>g</sup>Interfacial fracture between adhesive and glass sphere. <sup>h</sup>Interfacial fracture between adhesive and nanodecal.

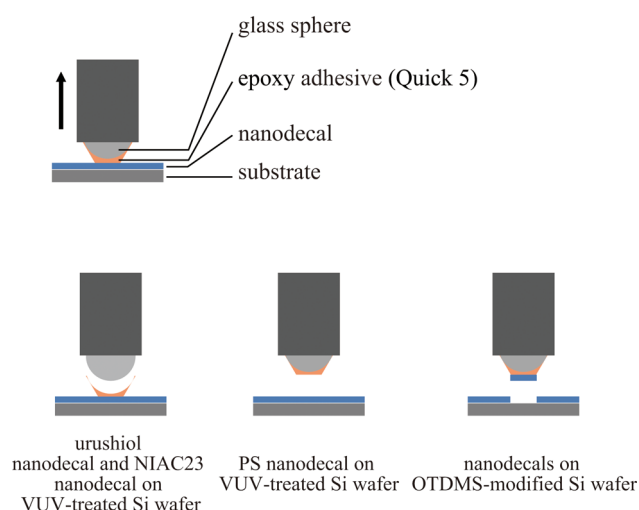


**Figure 3.** Schematic illustration of the fracture by pull-off adhesion test.

Because the value of fracture was about 6 MPa, the tensile adhesive strength of the cross-linked urushiol thin film is higher than this (Table 1). The strong adhesion was in good agreement with the tape test results. The adhesion strength was lower for the OTDMS-modified Si substrate (hydrophilic substrate) than for the VUV-treated substrate. The samples showed an interfacial fracture between the nanodecal and the substrate (Figure 3), and the adhesion strength was estimated as 1.53 MPa. However, this is still sufficient for practical use.

The capillary interaction is an effective driving force for the adhesion of materials in wet contact such as adhesion on hydrophilic substrates.<sup>30–32</sup> Generally, the capillary interaction is governed by the Laplace pressure and the surface tension. However, the contribution of the surface tension is negligible when the distance between two substrates is small enough.<sup>32</sup> In this case, the sum of the contact angles of the two substrates determined the direction and the strength of the interaction. When a cross-linked urushiol thin film (static water contact angle = 63°) was on a VUV-treated substrate (static water contact angle = 23°), the sum of the contact angle of these two surfaces was much smaller than 180°. As a result, an inward liquid meniscus was formed, which produced an attractive capillary interaction. The strength of capillary adhesion excluding the contribution of the surface tension can be estimated by

$$\text{capillary adhesion (MPa)} = \frac{\gamma_{LV}(\cos \theta_1 + \cos \theta_2)}{d} \quad (2)$$

Here,  $\gamma_{LV}$  is the surface energy of the liquid (for water  $\gamma_{LV} = 0.0728$  (N/m)) and  $\theta$  is the contact angle of the materials with the separation distance,  $d$  (Figure S8, Supporting Information). Because the separation distance is molecular scale with some fluctuation owing to their surface roughness, actual  $d$  value has, so far, been unclear. Therefore, a simple comparison between nanodecals cannot be done. However, the fact remains that hydrophilicity of cross-linked urushiol nanodecal have an big advantage for strong adhesion. For example, the adhesion strength is 1.5 times higher than that of PS nanodecal (static water contact angle = 92°) when the separation distance is simply consisted of two flat plates with a uniform, same separation distance.

It is known that catechol derivatives strongly adhere to various surfaces through hydrogen bonding and chelation.<sup>13–15</sup> It may also contribute the increase of adhesion strength. Therefore, the adhesion strength of NIAC23 thin film that has similar static water contact angle without catechol moiety was evaluated. Unfortunately, however, the difference was unclear from these experiments because NIAC23 also showed interfacial delamination between the glass sphere and the epoxy adhesive (Figure 3). The capillary interaction is enough strong to produce practical adhesion strength.

The van der Waals interaction (van der Waals adhesion) is the driving force for the adhesion of materials on hydrophobic substrates such as OTDMS-modified Si substrate because there is no specific interaction between them. The adhesion is calculated by the following equation:<sup>33</sup>

$$\text{van der Waals adhesion (MPa)} = -\frac{A}{6\pi d^3} \quad (3)$$

Here,  $A$  is the Hamaker constant, which is obtained from the dielectric constant, refractive index, and electronic absorption frequency of the materials. The Hamaker constant was calculated as  $7.60\text{--}7.70 \times 10^{-20}$ ,  $7.75 \times 10^{-20}$ , and  $7.03\text{--}7.14 \times 10^{-20}$  for cross-linked urushiol, PS, and NIAC23 nanodecals on OTDMS-modified Si substrate, respectively (see the Supporting Information). The order was in good agreement with that of the actual measured value of adhesion strength on OTDMS-modified Si substrate by pull-off adhesion test.

Interestingly, the adhesion strength decreased to 0.87 MPa when the thickness of the cross-linked urushiol thin film was increased to 1050 nm. Because films showed a similar surface roughness and static water contact angle (Table 1), the difference in the surface properties was negligible. Although the Young's modulus was also similar, the flexural rigidity of the materials decreased when their thickness was on the nanometer scale,<sup>9</sup> which allowed the nanodecal to deform to the surface topography of the substrate. As a result, the effective contact area per apparent unit was near the ideal contact area for producing strong adhesion. In contrast, the thick film could not deform to the surface topography because of its poor flexibility. Therefore, the thick film had a small contact area that produced weak adhesion.

The cross-linked urushiol nanodecals detached from VUV-treated Si substrate when they were soaked in water. The detachment was initiated from the edge of the nanodecals. The penetration of water into the interface caused the increase of separation distance to reduce the capillary interaction. The detachment was also observed under high humidity over 90%. However, strong adhesion was recovered when humidity was reduced again. Strong adhesion was achieved even for relative humidity close to 0%. The removal of water molecules at the interface is difficult, and the capillary interaction occurs between the nanodecal and hydrophilic substrates. When the sample was soaked in other solvents such as ethanol and acetone, no delamination was observed after 24 h. The strong adhesion remained intact even in acidic (*p*-toluenesulfonic acid solution in ethanol) and alkaline (potassium hydroxide solution in ethanol) solutions. The reversible attachment/detachment behavior was observed only when of nanodecals on VUV-treated Si substrate were treated with water. The nanodecal on a OTDMS-modified Si substrate showed strong adhesion in water after 24 h. It may arise from the difficulty of the penetration of water into the hydrophobic interface. However, these nanodecals were delaminated in ethanol and acetone. The

small Hamaker constants in these solvents ( $8.94 \times 10^{-21}$  and  $8.92 \times 10^{-21}$  for ethanol and acetone) probably contributed to the decrease of the adhesion.

Interestingly, urushiol thin film on VUV-treated Si wafer required over 24 h to complete the detachment in water; whereas NIAC23 and PS thin films were detached within a few hours. Because detachments proceeded in a similar way, the slow detachment of urushiol nanodecal over other nanodecals may arise from the difference of the adhesion mechanism. Capillary interaction that is the main driving force of the adhesion was immediately weakened by the soaking in water. However, the hydrogen bonding still acted in water. This is why the detachment of urushiol nanodecal was slowly progressed. This experimental results may prove the contribution of the hydrogen bonding for the adhesion of catechol derivatives urushiol.

**3.3. Fabrication of Functional Nanodecals.** As a simple example of a functional nanodecal, the surface of an urushiol thin film was textured by using a thermal imprinting technique. A  $2.3 \mu\text{m}$  thick urushiol film was thermally cured while it was pressed in a patterned mold, and the patterned nanodecal was transferred to another substrate. As confirmed by SEM observation, pillared structures  $2 \mu\text{m}$  in diameter with  $1 \mu\text{m}$  height were obtained over the imprinted area, which replicated the hole pattern of the corresponding Si mold (Figure S9, Supporting Information). Figure 4a shows a digital photograph of a surface-textured urushiol thin film attached to a Si substrate. The sample was transferred without any damage. Because the mold is iridescent due to the photonic effect of the periodic structures on the surface, the nanoimprinted object is equally iridescent. The patterned urushiol thin films showed different interference colors, which depended on the viewing angle. Raden is a Japanese decoration technique in which iridescent mother-of-pearl is inlaid in urushi-ware. Raden is highly prized technique; however, it requires time and effort, even for skilled artisans. It is interesting that an iridescent color was obtained through simple thermal imprinting process of glossy urushiol nanodecal.

Table 2 summarizes the wetting characteristics of the surface-textured urushiol nanodecal and those of samples fabricated directly on the Si substrate. No major differences were observed between the two. The wettability was unchanged by the decal-like transfer of the film, as we have reported previously.<sup>8</sup> The texturing of the surface can control the wettability of materials.<sup>7,22</sup> When a nanodecal was textured with a  $5 \mu\text{m}$  line-and-space pattern  $5 \mu\text{m}$  high, the CA values of the sample were anisotropic depending on the tilt direction ( $77^\circ$  for parallel, and  $134^\circ$  for orthogonal). The contact angle hysteresis ( $\Delta\theta$ ) was calculated as  $57^\circ$ . The strong anisotropic wetting could be useful for various applications, such as microfluidic devices, evaporation-driven alignment of materials, inkjet techniques, and easy-clean coatings.<sup>34</sup>

In addition to direct functionalization such as surface-texturing, nanodecals can also be used as a scaffold for functional materials. For example, the decal-like transfer of thin metal layers is usually impossible because they are too brittle, and only thick metal layers can be transferred. However, using mechanically robust nanodecal enables the transfer of thin metal layers. Figure 4b shows a digital photograph of a 60 nm thick cross-linked urushiol nanodecal bearing a 130 nm thick Au layer on its surface. The Au layer was created by selective vacuum deposition prior to the decal-like transfer, by using a polypropylene film as the deposition mask. The sample was

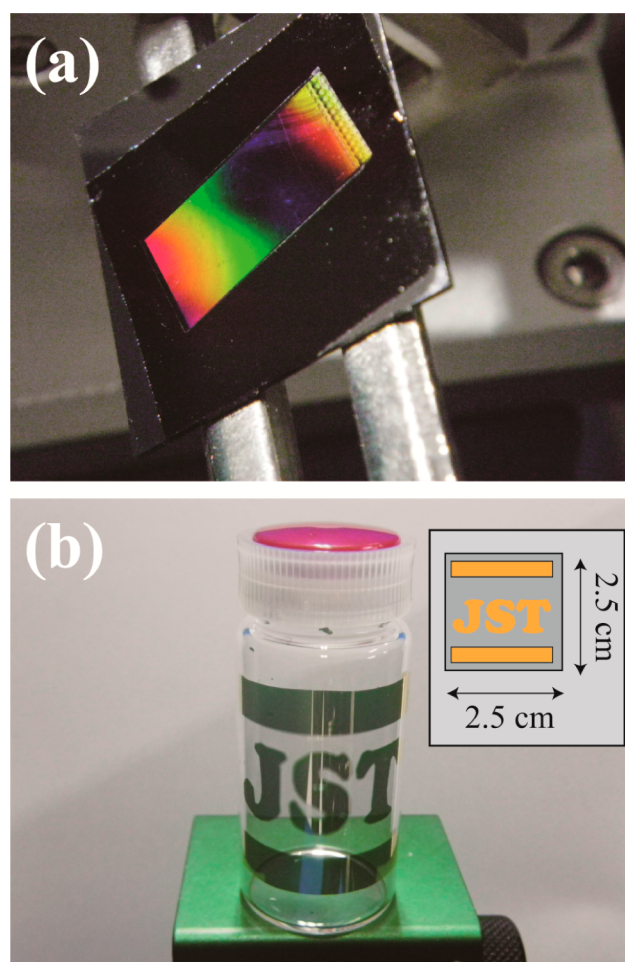


**Figure 4.** Digital photographs of (a) surface-textured urushiol nanodecal on a Si substrate, and (b) Au layer deposited on a 60 nm thick urushiol nanodecal on the curved surface of a glass vial.

transferred to the surface of a glass vial without any damage. Because the nanodecal acts as a scaffold like flexible substrates, the shape of Au layer is maintained during the transfer process. The transfer of an Au thin film by itself was unsuccessful and the film fragmented into small pieces during the process. Fragmentation also happened when a PS thin film was used as the scaffold. Thus, the robustness of the cross-linked urushiol nanodecal helps to maintain the morphology of the Au layer.

The electrochemical properties of the nanodecals were examined by using a potentiostat/galvanostat system. The nanodecals were measured after they were transferred to an ITO-coated glass slide. The output leakage current of the 60 nm thick urushiol nanodecal was about  $29 \mu\text{A}$  at 0.5 V (Figure 5). The electrical resistivity was calculated as  $2.04 \times 10^7 \Omega\cdot\text{cm}$ . The value was independent of the thickness of the nanodecal, and was almost same as that of the sample directly fabricated on the substrate. This indicates that the electrochemical properties of the nanodecal are not changed even after it is transferred to a different substrate, probably because of its macroscopic robustness. Moreover, the electrical resistivity in the  $z$ -direction remained intact even after the Au deposition (Figure 5). The Au decal showed good in-plane conductivity in the direction of the Au layer. Dekker and co-workers reported a decal-like attachment of nanostructures such as patterned metallic nanostructures.<sup>35</sup> Nanostructures on a hydrophilic substrate was overcoated with a hydrophobic polymer to detach the

Table 2. Wettability of Thin Films

sample	pattern	$\theta_s$ (deg) <sup>a</sup>	$\theta_a$ (deg) <sup>b</sup>	$\theta_r$ (deg) <sup>c</sup>	hysteresis (deg) <sup>d</sup>	sliding angle (deg)
nanodecal	flat <sup>e</sup>	63	71	49	22	17
	pillar (para) <sup>f</sup>	90	98	81	17	16
	pillar (ortho) <sup>f</sup>	110	109	102	7	17
	L&S (para) <sup>g</sup>	77	80	68	12	6
	L&S (ortho) <sup>g</sup>	134	156	87	69	<80
direct	flat <sup>e</sup>	67	75	54	21	20
	pillar (para) <sup>f</sup>	92	103	80	23	26
	pillar (ortho) <sup>f</sup>	117	112	106	6	15
	L&S (para) <sup>g</sup>	75	78	65	12	8
	L&S (ortho) <sup>g</sup>	98	107	58	49	<80

<sup>a</sup>Static water contact angle. <sup>b</sup>Advancing contact angle. <sup>c</sup>Receding contact angle. <sup>d</sup>Contact angle hysteresis ( $\theta_r - \theta_a$ ). <sup>e</sup>Pressed in a flat Si mold. <sup>f</sup>5  $\mu\text{m}$  pillared patterns with 5  $\mu\text{m}$  height. <sup>g</sup>5  $\mu\text{m}$  line-and-space pattern with 5  $\mu\text{m}$  height.

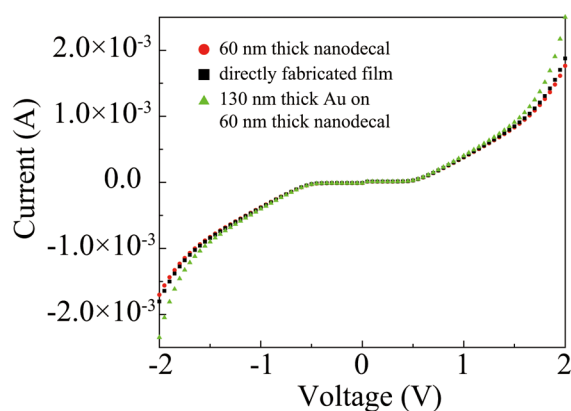


Figure 5. Output leakage current curves for 60 nm thick urushiol films: nanodecal (circles), directly fabricated film (squares), and 130 nm thick Au layer on a nanodecal (triangles).

structure from substrates onto water surface. They called the method “wedging transfer” because water acts as a wedge to detach the nanostructure. The design of a well-balanced surface energy is the key to inducing the detachment of nanostructures. Such optimization of experimental conditions is also necessary for conventional direct surface functionalization because surface conditions are different in each substrate. On the other hand, our indirect surface functionalization method does not require any optimization during surface functionalization because the nanodecal acts as an inert skin to adhere functional materials on various substrates. Moreover, the “wedging transfer” requires dissolution of overcoated polymer after the transfer of a nanostructure onto other substrates. Otherwise, surface properties such as in-plane conductivity in the direction of the nanostructure layer is hindered with the thick polymer layer. In contrast, as demonstrated in this paper, our method does not require the removal of the scaffold to obtain functionalize the surface.

Interestingly, the Au decal sample strongly adhered to the substrates. No delamination of the Au layer was observed in the tape test. Tautz and co-workers demonstrated that the interaction between gold (100) and *l*-DOPA is originated from the charge transfers (chemical interaction), the polarizability of the  $\pi$ -electron system (physisorption), or a combination of both between the catechol ring with the metal surface.<sup>36</sup> It may also act between deposited Au and urushiol nanodecals. Because metal layers do not usually adhere to substrates, an adhesive interlayer is required.<sup>37–39</sup> For example, Cu layers fabricated by electroless plating are adhered

to surfaces through a ZnO interlayer.<sup>37</sup> Electroless plating is used to deposit a metal thin layer on various surfaces.<sup>40</sup> Although the technique can deposit a metal layer on plastics, waste treatment is a major environmental problem. The decal-like transfer of metal thin films on urushiol could be used for the environmentally friendly deposition of metal thin layers on various substrates.

Salvatore and co-workers demonstrated a decal-like attachment of flexible electronic circuits.<sup>41</sup> They used parylene as the scaffold layer, and electronic circuits were fabricated on it through conventional process. Because the layer was formed on water-soluble poly(vinyl alcohol) layer, the electronic circuits on parylene can be transferred to any object after the detachment on water surface. It is certain that a 1  $\mu\text{m}$  thick parylene thin film is robust enough to maintain the film morphology during the processes. However, the use of thick scaffold layers may have some disadvantages for some practical use because the scaffold layers should be uninvolved in physical properties except surface properties. The contribution of a nanodecal on physical properties becomes smaller as the thickness decrease.<sup>8</sup> This is why a thin scaffold layer such as the urushiol nanodecal is indispensable. Moreover, as demonstrated above, the use of a thinner nanodecal is a simple solution to increase the adhesion on substrates. Therefore, the urushiol nanodecal, which shows robustness even on a nanometer thickness scale, has a big advantage as a nanodecal. Otherwise, films are damaged easily according to the decrease of the thickness, just we observed in PS and PDA thin films.

#### 4. CONCLUSIONS

We have demonstrated the surface functionalization of substrates using urushiol nanodecals. Urushiol is suitable for nanodecals because of its superior adhesive properties and high mechanical robustness. We surface textured a nanodecal using thermal imprinting, and showed that attaching the textured nanodecal altered the wettability of the surface in a similar to a directly fabricated film. We also used a nanodecal as a scaffold for an Au layer. The mechanical robustness of urushiol maintained the morphology of Au layer. Since urushiol has the advantage of good compatibility with other materials, the hybridization of functional materials is also candidate for fabricating functional nanodecals. For example, a tough composite of urushi and diatomite is used in some urushiware. This nanocomposite material has been used as a coating since the end of the 16th century in Japan. Because urushiol is a promising natural curing material that is consistent with the responsible resource management necessary for sustainable

living, the decal-like transfer of urushiol thin film for the fabrication of unique functional surfaces will become a powerful means as a surface modification technique using biobase materials.

## ■ ASSOCIATED CONTENT

### Supporting Information

Pull-off adhesion test, determination of Young's modulus, surface morphology of cross-linked urushiol film, fabrication of PDA nanodecal, adhesion data of nanodecals, calculation procedure of capillary adhesion, determination of Hamaker constant, and surface texturing of cross-linked urushiol nanodecals. This material is available free of charge via the Internet at <http://pubs.acs.org>.

## ■ AUTHOR INFORMATION

### Corresponding Authors

\* Hirohmi Watanabe. E-mail: [h-watanabe@cstf.kyushu-u.ac.jp](mailto:h-watanabe@cstf.kyushu-u.ac.jp).

\* Atsushi Takahara. E-mail: [takahara@cstf.kyushu-u.ac.jp](mailto:takahara@cstf.kyushu-u.ac.jp).

### Author Contributions

H. Watanabe and A. Takahara contributed equally to this work.

### Notes

The authors declare no competing financial interest.

## ■ ACKNOWLEDGMENTS

The authors thank Prof. Dr. Hiroshi Jinnai (JST ERATO) for helpful discussion.

## ■ REFERENCES

- (1) Gennes, P.-G. d. In *Soft Interfaces*; Cambridge University Press: Cambridge, U. K., 1994.
- (2) Genzer, J.; Efimenko, K. Creating Long-Lived Superhydrophobic Polymer Surfaces through Mechanically Assembled Monolayers. *Science* **2000**, *290*, 2130–2133.
- (3) Li, M.; Zhai, J.; Liu, H.; Song, Y. L.; Jiang, L.; Zhu, D. B. Electrochemical Deposition of Conductive Superhydrophobic Zinc Oxide Thin Films. *J. Phys. Chem. B* **2003**, *107*, 9954–9957.
- (4) Conrad, J. R.; Radtke, J. L.; Dodd, R. A.; Worzala, F. J.; Tran, N. C. Plasma Source Ion-Implantation Technique for Surface Modification of Materials. *J. Appl. Phys.* **1987**, *62*, 4591–4596.
- (5) Zhai, L.; Cebeci, F. Ç.; Cohen, R. E.; Rubner, M. F. Stable Superhydrophobic Coatings from Polyelectrolyte Multilayers. *Nano Lett.* **2004**, *4*, 1349–1353.
- (6) Zhang, G.; Wang, D. Y.; Gu, Z. Z.; Mohwald, H. Fabrication of Superhydrophobic Surfaces from Binary Colloidal Assembly. *Langmuir* **2005**, *21*, 9143–9148.
- (7) Honda, K.; Morita, M.; Masunaga, H.; Sasaki, S.; Takata, M.; Takahara, A. Room-Temperature Nanoimprint Lithography for Crystalline Poly(fluoroalkyl acrylate) Thin Films. *Soft Matter* **2010**, *6*, 870–875.
- (8) Watanabe, H.; Fujimoto, A.; Takahara, A. Manipulation of Surface Properties: The Use of Nanomembrane as a Nanometre-Thick Decal. *Soft Matter* **2011**, *7*, 1856–1860.
- (9) Watanabe, H.; Fujimoto, A.; Takahara, A. Concealing Surface Topography by Attachment of Nanometre-Thick Film. *Langmuir* **2013**, *29*, 2906–2911.
- (10) Watanabe, H.; Kunitake, T. A Large, Freestanding, 20 nm Thick Nanomembrane Based on an Epoxy Resin. *Adv. Mater.* **2007**, *19*, 909–912.
- (11) Watanabe, H.; Ohzono, T.; Kunitake, T. Fabrication of Large, Robust Nanomembranes from Diverse, Cross-Linked Polymeric Materials. *Macromolecules* **2007**, *40*, 1369–1371.
- (12) Watanabe, H.; Muto, E.; Ohzono, T.; Nakao, A.; Kunitake, T. Giant Nanomembrane of Covalently-Hybridized Epoxy Resin and Silica. *J. Mater. Chem.* **2009**, *19*, 2425–2431.
- (13) Crisp, D. J.; Walker, G.; Young, G. A.; Yule, A. B. Adhesion and Substrate Choice in Mussels and Barnacles. *J. Colloid Interface Sci.* **1985**, *104*, 40–50.
- (14) Dalsin, J. L.; Hu, B. H.; Lee, B. P.; Messersmith, P. B. Mussel Adhesive Protein Mimetic Polymers for the Preparation of Nonfouling Surfaces. *J. Am. Chem. Soc.* **2003**, *125*, 4253–4258.
- (15) Fan, X. W.; Lin, L. J.; Dalsin, J. L.; Messersmith, P. B. Biomimetic Anchor for Surface-Initiated Polymerization from Metal Substrates. *J. Am. Chem. Soc.* **2005**, *127*, 15843–15847.
- (16) Kohri, M.; Shinoda, Y.; Kohma, H.; Nannichi, Y.; Yamauchi, M.; Yagai, S.; Kojima, T.; Taniguchi, T.; Kishikawa, K. Facile Synthesis of Free-Standing Polymer Brush Films Based on a Colorless Polydopamine Thin Layer. *Macromol. Rapid Commun.* **2013**, *34*, 1220–1224.
- (17) Majima, R. The Main Element of Japans. (I. Announcement.) - Urushiol and Urushiol Dimethyl Ether. *Ber. Dtsch. Chem. Ges.* **1909**, *42*, 1418–1423.
- (18) Tyman, J. H. P.; Matthews, A. J. Long-Chain Phenols 22. Compositional Studies on Japanese Lac (*Rhus vernicifera*) by Chromatography and Mass-Spectrometry. *J. Chromatogr.* **1982**, *235*, 149–164.
- (19) Kumanotani, J. Urushi (Oriental Lacquer) - A Natural Aesthetic Durable and Future-Promising Coating. *Prog. Org. Coat.* **1995**, *26*, 163–195.
- (20) Ikeda, R.; Tanaka, H.; Uyama, H.; Kobayashi, S. A New Crosslinkable Polyphenol from a Renewable Resource. *Macromol. Rapid Commun.* **2000**, *21*, 496–499.
- (21) Watanabe, H.; Fujimoto, A.; Takahara, A. Characterization of Catechol-Containing Natural Thermosetting Polymer “Urushiol” Thin Film. *J. Polym. Sci., Part A: Polym. Chem.* **2013**, *51*, 3688–3692.
- (22) Watanabe, H.; Fujimoto, A.; Takahara, A. Surface Texturing Of Natural “Urushi” Thermosetting Polymer Thin Films. *Polym. J.* **2014**, *46*, 216–219.
- (23) Watanabe, H.; Fujimoto, A.; Yamamoto, R.; Nishida, J.; Kobayashi, M.; Takahara, A. Scaffold for Growing Dense Polymer Brushes from a Versatile Substrate. *ACS Appl. Mater. Interfaces* **2014**, *6*, 3648–3653.
- (24) Kim, S.; Christenson, H. K.; Curry, J. E. N-Octadecyltriethoxysilane Monolayer Coated Surfaces in Humid Atmospheres: Influence of Capillary Condensation on Surface Deformation and Adhesion. *J. Phys. Chem. B* **2003**, *107*, 3774–3781.
- (25) Ding, X. F.; Zhou, S. X.; Gu, G. X.; Wu, L. M. A Facile and Large-Area Fabrication Method of Superhydrophobic Self-Cleaning Fluorinated Polysiloxane/TiO<sub>2</sub> Nanocomposite Coatings with Long-Term Durability. *J. Mater. Chem.* **2011**, *21*, 6161–6164.
- (26) Stafford, C. M.; Harrison, C.; Beers, K. L.; Karim, A.; Amis, E. J.; Vanlandingham, M. R.; Kim, H. C.; Volksen, W.; Miller, R. D.; Simonyi, E. E. A Buckling-based Metrology for Measuring the Elastic Moduli of Polymeric Thin Films. *Nat. Mater.* **2004**, *3*, 545–550.
- (27) Zhu, B.; Edmondson, S. Polydopamine-Melanin Initiators for Surface-Initiated ATRP. *Polymer* **2011**, *52*, 2141–2149.
- (28) Lee, H.; Dellatore, S. M.; Miller, W. M.; Messersmith, P. B. Mussel-Inspired Surface Chemistry for Multifunctional Coatings. *Science* **2007**, *318*, 426–430.
- (29) Yamamoto, H.; Sakai, Y.; Ohkawa, K. Synthesis and Wettability Characteristics of Model Adhesive Protein Sequences Inspired by a Marine Mussel. *Biomacromolecules* **2000**, *1*, 543–551.
- (30) Fortes, M. A. Axisymmetric Liquid Bridges between Parallel Plates. *J. Colloid Interface Sci.* **1982**, *88*, 338–352.
- (31) De Souza, E. J.; Brinkmann, M.; Mohrdieck, C.; Arzt, E. Enhancement of Capillary Forces by Multiple Liquid Bridges. *Langmuir* **2008**, *24*, 8813–8820.
- (32) De Souza, E. J.; Brinkmann, M.; Mohrdieck, C.; Crosby, A.; Arzt, E. Capillary Forces between Chemically Different Surfaces. *Langmuir* **2008**, *24*, 10161–10168.
- (33) Israelachvili, J. N. In *Intermolecular and Surface Forces*, 3rd ed.; Academic Press: Oxford, U. K., 2011; Chapter 13.
- (34) Xia, D. Y.; Brueck, S. R. J. Strongly Anisotropic Wetting on One-Dimensional Nanopatterned Surfaces. *Nano Lett.* **2008**, *8*, 2819–2824.

(35) Schneider, G. g. F.; Calado, V. E.; Zandbergen, H.; Vandersypen, L. M. K.; Dekker, C. Wedging Transfer of Nanostructures. *Nano Lett.* **2010**, *10*, 1912–1916.

(36) Weinhold, M.; Soubatch, S.; Temirov, R.; Rohlfing, M.; Jastorff, B.; Tautz, F. S.; Doose, C. Structure and Bonding of the Multifunctional Amino Acid L-DOPA on Au(110). *J. Phys. Chem. B* **2006**, *110*, 23756–23769.

(37) Yoshiki, H.; Alexandruk, V.; Hashimoto, K.; Fujishima, A. Electroless Copper Plating Using ZnO Thin Film Coated on a Glass Substrate. *J. Electrochem. Soc.* **1994**, *141*, L56–L58.

(38) Yu, Z. J.; Kang, E. T.; Neoh, K. G. Amidoximation of the Acrylonitrile Polymer Grafted on Poly(tetrafluoroethylene-co-hexafluoropropylene) Films and Its Relevance to the Electroless Plating of Copper. *Langmuir* **2002**, *18*, 10221–10230.

(39) Matsui, J.; Kubota, K.; Kado, Y.; Miyashita, T. Electroless Copper Plating onto Polyimide using Polymer Nanosheet as a Nano-Adhesive. *Polym. J.* **2007**, *39*, 41–47.

(40) Sullivan, M. V.; Eigler, J. H. Electroless Nickel Plating for Making Ohmic Contacts to Silicon. *J. Electrochem. Soc.* **1957**, *104*, 226–230.

(41) Salvatore, G. A.; Munzenrieder, N.; Kinkeldei, T.; Petti, L.; Zysset, C.; Strelbel, I.; Buthe, L.; Troster, G. Wafer-Scale Design of Lightweight and Transparent Electronics That Wraps around Hairs. *Nat. Commun.* **2014**, *5*, 8.